RSC Advances

PAPER

View Article Online
View Journal | View Issue

Cite this: *RSC Adv.*, 2025, **15**, 30339

The preparation of amphiphilic carbonaceous particle-derived membranes as a potent sterilant and anticoagulant

Wenxin Zhang,[a] Yanna Geng,[b] Mengke Wang,[b] Shuai Liu,[c] Xueping Wang,[c] Xiaoke Xu[c] and Qiang Wu *[c]

Objective: To synthesize and evaluate the function of antibacterial and anticoagulant properties of amphiphilic carbonaceous particle (ACP) derived polyurethane composite membranes TPU/ACPs-CS-PVS-Ag/ACPs-CS-Hep. *Methods*: ACPs, ACPs-CS, ACPs-CS-PVS-Ag, ACPs-CS-Hep and ACPs-CS-PVS-Ag/ACPs-CS-Hep were prepared and mixed with a TPU matrix, to assess the dispersibility respectively. The blank TPU, TPU/ACPs, TPU/ACPs-CS, TPU/ACPs-CS-PVS-Ag, TPU/ACPs-CS-Hep and TPU/ACPs-CS-PVS-Ag/ACPs-CS-Hep membranes were prepared. The hydrophilicity of these composite membranes was determined by *t* contact angle test. Their mechanical properties were measured by an electronic precision universal experimental machine. The antibacterial activity was detected by co-culturing the composite membrane and bacteria. The anticoagulant activity was evaluated by incubating the composite membrane with the anticoagulant blood. *Results*: ACPs, ACPs-CS, ACPs-CS-PVS-Ag, ACPs-CS-Hep and ACPs-CS-PVS-Ag/ACPs-CS-Hep were dispersed in the hydrophobic TPU matrix and formed uniform composite membranes with TPU matrix. The contact angles of blank TPU, TPU/ACPs, TPU/ACPs-CS, TPU/ACPs-CS-PVS-Ag, TPU/ACPs-CS-Hep, and TPU/ACPs-CS-PVS-Ag/ACPs-CS-Hep composite membranes were 103.2°, 97.5°, 87.2°, 86.9°, 81.8° and 84.7°, respectively, indicating that the hydrophilicity of the TPU membrane could be enhanced by functional ACPs. The tensile strength of the five composite membranes increased compared with the TPU control. Compared with blank TPU, TPU/ACPs, TPU/ACPs-CS and TPU/ACPs-CS-Hep membranes, the TPU/ACPs-CS-PVS-Ag and TPU/ACPs-CS-PVS-Ag/ACPs-CS-Hep membranes exhibited better antibacterial activity, as evidenced by reducing bacterial survival rate and adhesion after co-culture with *S. aureus*, *E. coli*, *C. albicans* and MRSA bacteria. The membranes of TPU, TPU/ACPs and TPU/ACPs-CS instead of TPU/ACPs-CS-Hep and TPU/ACPs-CS-PVS-Ag/ACPs-CS-Hep led to blood coagulation, validating the anticoagulant effect of ACPs-CS-Hep-based membranes. Compared with blank TPU, 1 wt% of TPU/ACPs-CS-Hep, TPU/ACPs-CS-PVS-Ag/ACPs-CS-Hep and 3 wt% of TPU/ACPs-CS-PVS-Ag/ACPs-CS-Hep membranes resulted in decreased platelet adhesion; TPU/ACPs-CS-PVS-Ag/ACPs-CS-Hep with 3 wt% showed stronger inhibition of platelet adhesion than the corresponding 1 wt% membrane, suggesting that ACPs-CS-Hep-based membranes had antiplatelet adhesion activity in a dose-dependent manner. *Conclusion*: The TPU/ACPs-CS-PVS-Ag/ACPs-CS-Hep membrane has been successfully synthesized and possessed excellent antibacterial and anticoagulant properties.

Received 14th March 2025
Accepted 4th June 2025

DOI: 10.1039/d5ra01833a

rsc.li/rsc-advances

1. Introduction

Catheter-associated infections and catheter-associated thrombosis are common diseases in medical procedures, both of which are related to the use of medical catheters for intravenous infusion, central venous catheterization, and blood transfusion.[1,2] Colonization of pathogens is the main cause of catheter-associated infections. Bacteria on the surface of the catheter and in the cavity of the catheter are transmitted through the blood and then cause infections.[3] Statistics indicated that, more than half of the catheter surface pathogen-caused infections are induced by Gram-positive bacteria in hemodialysis patients, most commonly *Staphylococcus aureus* (*S. aureus*); the remaining infections are caused by Gram-negative bacteria, such as *Escherichia coli* (*E. coli*).[4] The occurrence of catheter-associated infections is closely related to the biomembrane on the surface of the catheter. The bacteria on the surface of the material can secrete exopolysaccharides,

[a]*The First Affiliated Hospital of the Henan University of Traditional Chinese Medicine, Zhengzhou, China*

[b]*Department of Pharmacy, Huaihe Hospital of Henan University, Kaifeng, China*

[c]*School of Pharmacy, Henan University, Kaifeng, China. E-mail: henuwuqiang@henu.edu.cn*

which are beneficial to the adhesion of neighboring bacteria. Long-term use of antibiotics can make bacteria resistant to drugs and even lead to the emergence of superbugs.[5] When the catheter comes into contact with blood, platelets and plasma proteins quickly adhere to the surface material, and subsequently platelets can activate the coagulation system, thereby leading to the occurrence of thrombus.[6] The traditional antibacterial and anticoagulant approaches include the coating of antibacterial agent and anticoagulant heparin to the catheter, which has certain effects but has simultaneously some disadvantages such as short action time, poor efficacy and inconvenient use. Therefore, it is of the essence to exploit novel antibacterial and anticoagulant biological functional materials to develop more effective methods to prevent the occurrence of catheter-related infections and catheter-related thrombosis.

Heparin (Hep), a common anticoagulant preparation in clinical, can combine with antithrombin III and thus inhibits the formation of thrombosis. The biological materials containing Hep can effectively prolong blood coagulation time.[7] Although silver ion has a strong bactericidal effect, it is easy to cause harm to the human body, so the present research mainly focuses on nano-silver and silver-carrying antibacterial materials.[8] Thermoplastic polyurethane (TPU) is a copolymer formed by polymerization of isocyanate, polyol and small molecule chain extender, which has been widely used as a catheter material, showing advantaged of water resistance, oxidation resistance, and good histocompatibility.[9]

In our previous study,[10] we have prepared Hep/CS functionalized ACPs and silver nanoparticles (PVS-Ag) modified ACPs to obtain ACPs-CS-PVS-Ag and ACPs-CS-Hep with various biological properties, including antimicrobial activity, anticoagulant activity, and good blood compatibility and biocompatibility. In this work,we sought to combine the generated biological carbon materials with TPU matrix to synthesize the functional composite membranes. Further, we elucidated the antimicrobial and anticoagulant properties of the composite membranes. Our study provides new ideas in preventing catheter-related infections and catheter-related thrombosis.

2. Experimental

2.1 Materials

Budding yeast *Saccharomyces cerevisiae* (*S. cerevisiae*) was purchased from Angel Yeast (Qingdao, China). *Staphylococcus aureus* (*S. aureus*), *Escherichia coli* (*E. coli*), *Candida albicans* (*C. albicans*) and methicillin-resistant *Staphylococcus aureus* (MRSA) were purchased from ATCC (Manassas, VA, USA). TPU elastomer rubber was obtained from Suzhou Yunzhan Plastics Co., Ltd (Suzhou, China). *N*,*N*-dimethylformamide (DMF) was purchased from Tianjin Fusi Chemical Reagent Co., Ltd (Tianjin, China), and nutrition agar was procured from Beijing Obstar Biotechnology Co., Ltd (Beijing, China). Human blood samples were residual specimens remaining after routine clinical testing, obtained from Huaihe Hospital of Henan University. Human blood samples were residual specimens remaining after routine clinical testing, obtained from Huaihe Hospital of Henan University. Hospital clinicians collected venous blood during standard clinical care for diagnostic purposes. Researchers identified patients with normal coagulation function through the Hospital Information System (HIS), and then utilized residual blood samples remaining after clinical testing. All other reagents were of analytical grade.

2.2 Membrane preparation

2.2.1 Preparation of ACPs. 50 g of brewed yeast was added in 200 mL of deionized water. After thorough mixing, incubation was allowed for 10 min at room temperature, followed by the filtration and purification through filter papers and centrifugation for 3 min at 8000 rpm. After removing the supernatant, the precipitates were re-suspended in acetone solution and then shook in a shaker for 20 min, and these procedures were repeated twice. After being washed three times with deionized water, the precipitates were mixed with phosphate-buffered saline (PBS, Solarbio, Beijing, China) containing 2% glutaral and then transferred to the reactor. After 12 h of incubation in water at 180 °C, the upper floating materials were discarded, and the precipitates were fully washed until no black sediment was washed out. Following centrifugation, the precipitates were harvested, dried, and named ACPs (a yellow fine powder).

2.2.2 Preparation of ACPs-CS. 150 mg of ACPs were homogenized in 40 mL of PBS (pH = 5.3) by ultrasonography. Meantime, 100 mg of carboxyl activators EDC and NHC were dissolved in 10 mL of PBS (pH = 5.3). The above two solutions were mixed and incubated for 2 h in a shaking machine at 180 rpm at room temperature. After that, 200 mg of CS dissolved in 1% CH_3COOH solution was added into the carboxyl activated ACPs and applied overnight at 180 rpm at room temperature. After centrifugation, the precipitates were washed twice with 1% CH_3COOH solution for removing the uncombined CS and then washed twice with deionized water to remove the CH_3COOH, which was followed by washing with absolute ethyl alcohol. The precipitates were subjected to vacuum drying to obtain a light yellow fine powder (named ACPs-CS).

2.2.3 Preparation of ACPs-CS-PVS-Ag. 16.9 mg of $AgNO_3$ was dissolved in 46 mL of deionized water in a brown glass bottle. 10 μL of 10% PVS was added into 2 mL of deionized water and then was slowly added into the $AgNO_3$ solution, followed by stir of 20 min. After that, 3.78 mg of $NaBH_4$ dissolved in 2 mL of deionized water was also was slowly added into the $AgNO_3$ solution to obtain tawny PVS-Ag. The mixture of 60 mg ACPs-CS and 36 mL PVS-Ag solution was prepared and incubated for 8 h in the dark at room temperature. After centrifugation for 3 min at 8000 rpm, the supernatant was removed, and the precipitates were washed with deionized water until colorless. A 6-h incubation was performed in a drying cabinet (Shuliyiqi, Shanghai, China) at 60 °C, and the functional amphiphilic biomaterial ACPs-Cs-PVS-Ag carrying PVS-Ag were obtained.

2.2.4 Preparation of ACPs-CS-Hep. 25 mg of Hep sodium dissolved into 50 mL of 0.1 M PBS (pH 5.3) was supplemented with 50 mg of EDC and NHS and incubated for 1 h. 50 mg of ACPs-CS was then added into 30 mL of Hep sodium solution and applied for 24 h at 4 °C in the dark. After centrifugation for 3 min at 8000 rpm, the precipitates were washed with deionized

water until colorless and then washed with absolute ethyl alcohol, followed by drying for 6 h at 60 °C to obtain the functional amphiphilic biomaterial ACPs-CS-Hep carrying Hep.

2.2.5 Preparation of composite membranes. According to the experimental requirements, the suitable weight of biological carbon composite materials ACPs, ACPs-CS, ACPs-CS-PVS-Ag, ACPs-CS-Hep and ACPs-CS-PVS-Ag/ACPs-CS-Hep in a centrifuge tube was added with 5 mL of DMF, respectively. After homodisperse by ultrasonography, each of the composite materials was added in 4.95 g of TPU in a brown glass bottle. The centrifuge tube was washed three times with 20 mL of DMF, which also was added into the brown glass bottle containing TPU. After sealing and stir for 5 h, 5 mL of the mixture of TPU matrix and biological carbon composite materials was placed in a 40 mm Petri dish. The air bubbles on the surface were removed by vacuuming, and the Petri dish was sealed with plastic wrap, which had small holes punched by needle tips to prevent dust from falling into the dish and slow down the evaporation rate. After drying for 6 h at 55 °C, the following TPU membranes were stored at 4 °C until use: TPU/ACPs, TPU/ACPs-CS, TPU/ACPs-CS-PVS-Ag, TPU/ACPs-CS-Hep and TPU/ACPs-CS-PVS-Ag/ACPs-CS-Hep composite membranes. The composite membranes with different mass percentage (wt%) were prepared in accordance to the experimental requirements. Mass percentage (wt%) = 100% × the quality of the biological carbon composite material ÷ (total quality of the composite biological carbon material + TPU matrix).

2.3 Evaluation of dispersibility of the generated bio-carbon composite materials in TPU

Equal amounts of ACPs, ACPs-CS, ACPs-CS-PVS-Ag, ACPs-CS-Hep and ACPs-CS-PVS-Ag/ACPs-CS-Hep were added in equal amounts of TPU matrix, respectively. After addition of the appropriate volume of DMF, the mixture was homogenized, and images were photographed to record the dispersion.

2.4 Measurement of the surface contact angle of the generated composite membranes

The synthesized TPU blank, TPU/ACPs, TPU/ACPs-CS, TPU/ACPs-CS-PVS-Ag, TPU/ACPs-CS-Hep and TPU/ACPs-CS-PVS-Ag/ACPs-CS-Hep composite membranes were cut into the size of 0.5 cm × 1 cm and washed with deionized water, followed by placement on the glass slide. The surface contact angle of the membranes was measured. The detection was performed with five independent replicates, and data with error less than 5% were used to evaluate the contact angle value and expressed as mean ± standard error. According to the contact angle of 90° as the fiducial value, the lipophilicity enhanced with the increase of the contact angle (>90°), and the hydrophilicity enhanced with the decrease of the contact angle (<90°).

2.5 Detection of mechanical properties of the generated composite membranes

Using a ASTM-C dumbbell cutter, the synthesized TPU blank, TPU/ACPs, TPU/ACPs-CS, TPU/ACPs-CS-PVS-Ag, TPU/ACPs-CS-Hep and TPU/ACPs-CS-PVS-Ag/ACPs-CS-Hep composite membranes were cut into the shape of dumbbells and subsequently placed on an electronic precision universal experimental machine with a tensile speed of 20 mm min^{-1}. Evaluation of mechanical properties was performed by pulling cut the membranes and recording the tensile strength and the elongation at break of the membrane. The measurement was carried out with five independent replicates, and data with error less than 5% were used to evaluate the tensile strength and the elongation at break and expressed as mean ± standard error.

2.6 Evaluation of antibacterial activity of the generated composite membranes

The synthesized blank TPU, TPU/ACPs, TPU/ACPs-CS, TPU/ACPs-CS-PVS-Ag, TPU/ACPs-CS-Hep and TPU/ACPs-CS-PVS-Ag/ACPs-CS-Hep composite membranes were cut, washed three times with PBS, and sterilized by ultraviolet radiation. These sterile membranes were then placed in 6 mL of *S. aureus*, *E. coli*, *C. albicans* and MRSA bacterial solution (1×10^5 CFU mL^{-1}), respectively, and incubated for 6 h in an incubator (Center Weiye Co., Ltd, Beijing, China) at 150 rpm at 37 °C, followed by collection of the bacterial solution. 100 μL of the bacterial solution was added to the solidified nutrient agar in culture dishes, coated evenly, sealed by sealing membranes, and incubated at 37 °C for 24 h. The antibacterial activity was determined by observing the bacterial growth and analyzing the survival rate. The treatment without membrane was used as the control.

The composite membranes cultured in the bacterial solution were washed five times to remove the non-adhered bacteria and dried in a sterile environment. The treated membranes were then placed on solidified nutrient agar in culture dishes, and a small amount of nutrient agar medium was added to slightly cover the membranes. After solidification and seal, a 24-h culture was allowed at 37 °C. The number of colonies on the surface of the membrane was counted. The lower the number of colonies suggested the stronger the resistance to bacterial adhesion on the membrane surface.

2.7 Evaluation of anticoagulant activity of the generated composite membranes

Human blood samples were residual specimens remaining after routine clinical testing, obtained from Huaihe Hospital of Henan University. Hospital clinicians collected venous blood during standard clinical care for diagnostic purposes. Researchers identified patients with normal coagulation function through the Hospital Information System (HIS) and then, following receipt of informed consent, utilized residual blood samples remaining after clinical testing. The synthesized blank TPU, TPU/ACPs, TPU/ACPs-CS, TPU/ACPs-CS-Hep and TPU/ACPs-CS-PVS-Ag/ACPs-CS-Hep composite membranes were cut into the square of 10 mm side length. 100 μL of human fresh anticoagulant blood was added onto the sheared membranes before addition of 0.2 M of 10 μL $CaCl_2$. After mixing, incubation was performed for 10, 20, 30, 40, 50, and 60 min. Subsequently, the composite membranes were placed in 50 mL distilled water and incubated for 10 min. Hemolysis reaction

could occur on blood cells without coagulation, and ruptured blood cells released hemoglobin into the deionized water. The absorbance was detected at 540 nm by a microplate reader. The high absorbance value was proportional to the strong anticoagulant activity.

2.7.1 Platelet adhesion experiment. Fresh anticoagulant blood samples were centrifuged at 1500 rpm for 15 min to obtain platelet-enriched plasma. The synthesized blank TPU, TPU/ACPs, TPU/ACPs-CS, TPU/ACPs-CS-Hep and TPU/ACPs-CS-PVS-Ag/ACPs-CS-Hep composite membranes were cut into the square of 10 mm side length, dried, placed in the platelet-enriched plasma, and incubated for 2 h at 37 °C. The membranes were washed three times with normal saline to remove the non-adhered platelets and then fixed with 2.5% glutaraldehyde for 2 h. After that, the membranes were further washed three times with normal saline, dehydrated with different concentrations of ethanol, and dried at room temperature. The composite membranes were glued to the conductive adhesive and sprayed with gold. The platelet adhesion was observed by a scanning electron microscope (JEOL, Japan).

2.8 Hemolysis of ACPs-CS-Hep

1 mL of human blood was diluted 10 times with PBS and then centrifuged (10 000 rpm, 10 min) to obtain the red blood cells (RBCs) that was washed with PBS and dispersed into 5×PBS buffer. 0.2 mL of the diluted RBCs solution and 0.8 mL of the ACPs-CS-Hep solution with different concentrations (*i.e.* 0 μg mL^{-1}, 200 μg mL−1,400 μg mL^{-1}, 600 μg mL^{-1}, 800 μg mL^{-1}, and 1000 μg mL^{-1}) were homogenously processed by vortex oscillation, settled at room temperature for 3 h, and centrifuged (10 000 rpm, 3 min). Then the supernatant were collected with the absorbance at 570 nm measured, of which the absorbance at 655 nm was taken as control. The hemolysis ratio (%) was calculated as followed:

$$\text{Hemolysis ratio} = \frac{OD_{sample} - OD_{Negative\ control}}{OD_{Positive\ control} - OD_{Negative\ control}} \times 100\%$$

where, OD_{Sample}, $OD_{Negative\ control}$ or $OD_{Positive\ control}$ stands for the absorbance of the mixture of the ACPs-CS-Hep solution with different concentrations, the deionized water or PBS, and the diluted RBCs solution placed at room temperature for 3 h.

2.9 Cytotoxicity of ACPs-CS-Hep

Normal human liver cells HL-7702 were digested and centrifuged. 100 μL of the cell suspension was inculcated into the 96-well plate (5000 cells per well) and cultured for 24 h. Then 100 μL of the ACPs-CS-Hep solution with different concentrations (*i.e.* 0 μg mL^{-1}, 0.1 μg mL^{-1}, 1 μg mL^{-1}, 10 μg mL^{-1}, 100 μg mL^{-1}, and 1000 μg mL^{-1}) was added to each well, respectively. After 24 h, 20 μL methyl thiazolyl tetrazolium (MTT) solution was added to each well, mixed and cultured at 37 °C for 4 h. Subsequently, the plate was washed with PBS with 100 μL dimethyl sulfoxide (DMSO) added into each well, the absorbance of which at 490 nm was detected by microplate reader.

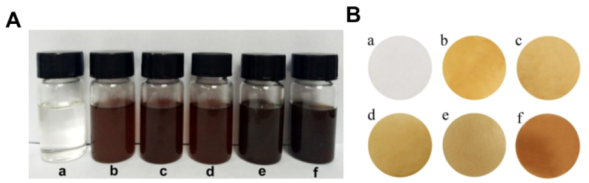

Fig. 1 Dispersibility (A) and membrane formation (B) of different APCs in TPU matrix. (a) represented the TPU blank matrix, (b) represented the mixture of the TPU matrix and ACPs, (c) represented the mixture of the TPU matrix and ACPs-CS, (d) represented the mixture of the TPU matrix and ACPs-CS-PVS-Ag, (e) represented the mixture of the TPU matrix and ACPs-CS-Hep, (f) represented the mixture of the TPU matrix, ACPs-CS-PVS-Ag and ACPs-CS-Hep.

3. Results

3.1 Identification of dispersibility and membrane formation of different APCs in TPU matrix

The detail characterization of ACPs, ACPs-CS, ACPs-CS-PVS-Ag, ACPs-CS-Hep and ACPs-CS-PVS-Ag/ACPs-CS-Hep was shown in our published literature.[10] As shown in Fig. 1A, ACPs, ACPs-CS, ACPs-CS-PVS-Ag, ACPs-CS-Hep, and ACPs-CS-PVS-Ag/ACPs-CS-Hep composite materials were uniformly dispersed in the hydrophobic TPU matrix, respectively. Moreover, the TPU matrix had no effect on the amphiphilicity of the ACPs materials (Fig. 1A). As expected, ACPs, ACPs-CS, ACPs-CS-PVS-Ag, ACPs-CS-Hep and ACPs-CS-PVS-Ag/ACPs-CS-Hep could form fine and symmetrical composite membranes with the TPU matrix, respectively (Fig. 1B).

3.2 Identification of hydrophilicity of the generated composite membranes

The hydrophilicity of the generated TPU membranes is determined by detecting the contact angle on the surface of the membranes, and the hydrophilicity increases with the decrease of the contact angle (<90°). The contact angle of the blank TPU membrane was 103.2°; the contact angle of the generated composite membranes diminished with the increase of the mass percentage (wt%) of ACPs in TPU matrix; when the content of ACPs in TPU matrix was 5.0 wt%, the contact angle of the composite membrane was 87.2° (Fig. 2A), indicating that these composite membranes have good hydrophilicity, and addition of ACPs can

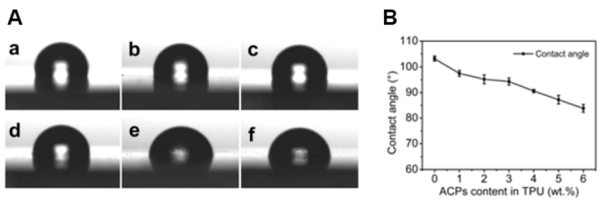

Fig. 2 Surface contact angle of the composite membranes. (A) Water contact angles and (B) corresponding value of TPU/ACPs composite membrane. (a) represented the TPU blank control membrane, (b) represented the TPU/ACPs membrane, (c) represented the TPU/ACPs-CS membrane, (d) represented the TPU/ACPs-CS-PVS-Ag membrane, (e) represented the TPU/ACPs-CS-Hep membrane, f represented the TPU/ACPs-CS-PVS-Ag/ACPs-CS-Hep membrane.

enhance the hydrophilicity of the TPU composite membranes. When the content of functional ACPs in TPU matrix was 1.0 wt%, the contact angles of blank TPU, TPU/ACPs, TPU/ACPs-CS, TPU/ACPs-CS-PVS-Ag, TPU/ACPs-CS-Hep, and TPU/ACPs-CS-PVS-Ag/ACPs-CS-Hep composite membranes were 103.2°, 97.5°, 87.2°, 86.9°, 81.8° and 84.7°, respectively (Fig. 2B). These results suggest that the hydrophilicity of the TPU composite membranes can be increased by functional biological carbon materials.

3.3 Identification of mechanical properties of the generated composite membranes

As shown in Fig. 3A, the tensile strength and the elongation at break of the TPU composite membranes varied with the addition of ACPs. With the increasing content of ACPs, the tensile strength and the elongation at break of the TPU composite membranes increased gradually at first and then decreased gradually; when the concentration of ACPs was 3.0 wt%, the generated composite films had the strongest tensile strength; when the concentration was 4.0 wt%, these composite films had the strongest elongation at break; the concentration of ACPs exceed 5.0 wt% did not affect the mechanical properties of the TPU composite membranes (Fig. 3A). When the content of different ACPs in TPU matrix was 1.0 wt%, the tensile strength of TPU/ACPs, TPU/ACPs-CS, TPU/ACPs-CS-PVS-Ag, TPU/ACPs-CS-Hep, and TPU/ACPs-CS-PVS-Ag/ACPs-CS-Hep composite membranes increased compared with the blank TPU control (Fig. 3B), demonstrating that functional ACPs can enhance the tensile strength of the TPU composite membranes. However, the 1.0 wt% addition of different ACPs did not markedly affect the elongation at break of the TPU composite membranes (Fig. 3B). All these results demonstrate that the generated ACPs can improve the mechanical properties of the TPU composite membranes.

3.4 Identification of antibacterial activity of the generated composite membranes

Compared with the TPU blank control, incubation of bacteria solution (*S. aureus*, *E. coli*, *C. albicans* and MRSA bacteria) with

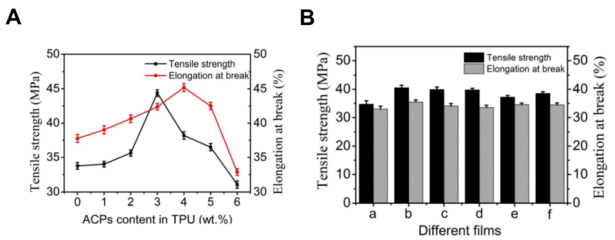

Fig. 3 Tensile strength and elongation at break of the composite membranes. (A) The tensile strength and elongation at break of the TPU/ACPs composite membrane carrying different amounts of ACPs. (B) Tensile strength and elongation at break of the composite membranes with bio-carbon materials. (a) represented the TPU blank control membrane, (b) represented the TPU/ACPs membrane, (c) represented the TPU/ACPs-CS membrane, (d) represented the TPU/ACPs-CS-PVS-Ag membrane, (e) represented the TPU/ACPs-CS-Hep membrane, (f) represented the TPU/ACPs-CS-PVS-Ag/ACPs-CS-Hep membrane.

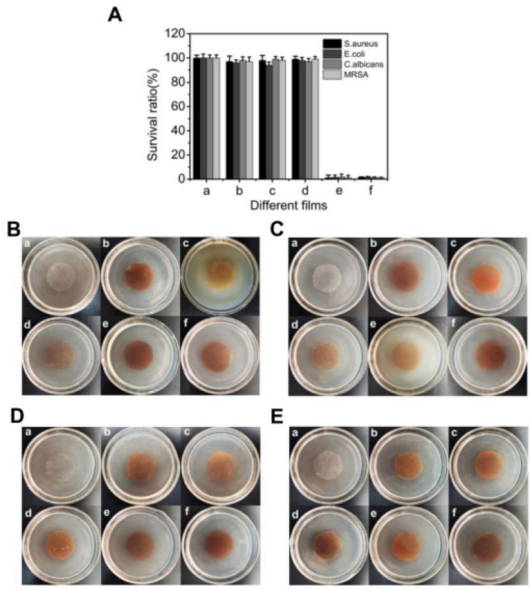

Fig. 4 Antibacterial activity of the composite membranes. (A–E) Antibacterial effect of the composite membranes (A), and antibacterial adhesion images of the composite membranes after incubation with solution of *S. aureus* (B), *E. coli* (C), *C. albicans* (D) and MRSA (E). (a) represented the TPU blank control membrane, (b) represented the TPU/ACPs membrane, (c) represented the TPU/ACPs-CS membrane, (d) represented the TPU/ACPs-CS-Hep membrane, (e) represented the TPU/ACPs-CS-PVS-Ag membrane, (f) represented the TPU/ACPs-CS-PVS-Ag/ACPs-CS-Hep membrane.

TPU/ACPs, TPU/ACPs-CS and TPU/ACPs-CS-Hep composite membranes did not significantly affect the bacterial survival rate in supernatants, while the TPU/ACPs-CS-PVS-Ag and TPU/ACPs-CS-PVS-Ag/ACPs-CS-Hep composite membranes strongly reduced the bacterial survival rate (Fig. 4A), indicating that the functional materials ACPs-CS-PVS-Ag have strong antibacterial activity. Consistently, after incubation with bacteria solution, there were more adhesive bacteria in the TPU blank, TPU/ACPs 1.0 wt%, TPU/ACPs-CS 1.0 wt% and TPU/ACPs-CS-Hep 1.0 wt% membranes; the TPU/ACPs-CS-PVS-Ag and TPU/ACPs-CS-PVS-Ag/ACPs-CS-Hep composite membranes had lower adhesive bacteria than the TPU blank control (Fig. 4B–D), suggesting that the functional materials ACPs-CS-PVS-Ag can repress the bacterial adhesion on the membrane surface.

3.5 Identification of anticoagulant activity of the generated composite membranes

After incubation of the generated composite membranes with human fresh anticoagulant blood samples, we found that blood clotting occurred in the TPU blank, TPU/ACPs, and TPU/ACPs-CS groups, as evidenced by the absorbance of less than 0.1 in these groups in the assayed time frame (10–60 min incubation) (Fig. 5A), showing that the blank TPU, TPU/ACPs, and TPU/ACPs-CS membranes had no anticoagulant effect. Although the absorbance of the TPU/ACPs-CS-Hep and TPU/ACPs-CS-PVS-Ag/ACPs-CS-Hep groups decreased in the assayed time frame, it remained greater than 0.1 (Fig. 5A), indicating that the blood

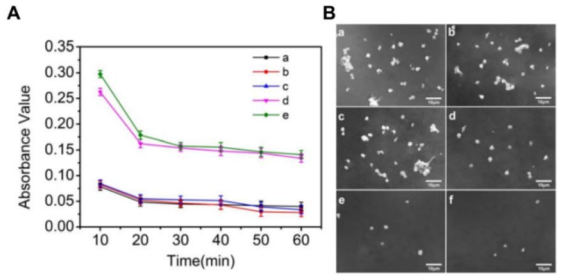

Fig. 5 Anticoagulant effect of the composite membranes. (A) Dynamic blood coagulation time curve of the composite membranes. (a) represented the TPU blank control membrane, (b) represented the TPU/ACPs membrane, (c) represented the TPU/ACPs-CS membrane, (d) represented the TPU/ACPs-CS-Hep membrane, (e) represented the TPU/ACPs-CS-PVS-Ag/ACPs-CS-Hep membrane. (B) SEM images of platelet adhesion of the composite membranes. (a) Represented the blank TPU membrane, (b) represented the TPU/ACPs membrane, (c) represented the TPU/ACPs-CS membrane, (d) represented the TPU/ACPs-CS-Hep membrane, (e) represented the TPU/ACPs-CS-PVS-Ag/ACPs-CS-Hep 1 wt% membrane, f represented the TPU/ACPs-CS-PVS-Ag/ACPs-CS-Hep 3 wt% membrane.

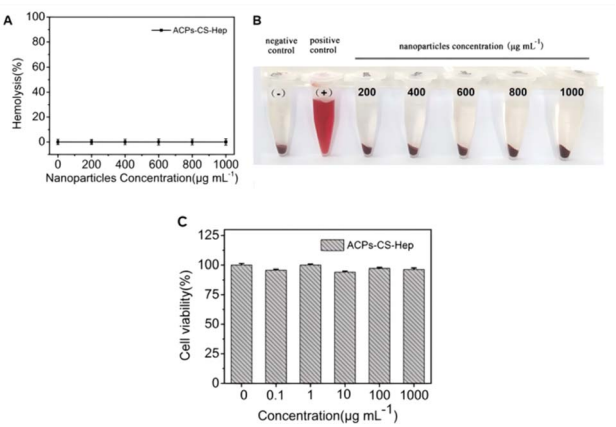

Fig. 6 ACPs-CS-Hep had excellent hemocompatibility. (A) Hemolysis assay of ACPs-CS-Hep. (B) Photograph of RBCs incubated with ACPs-CS-Hep under different concentrations for 3 h. (C) Cell viability of HL-7702 maintained in ACPs-CS-Hep under different concentrations for 24 h.

was not completely coagulated in the two groups. These results suggest that the composite membranes carrying ACPs-CS-Hep have anticoagulant activity.

After 3 h incubation, we observed a large number of platelets adhered to the TPU blank, TPU/ACPs, and TPU/ACPs-CS membranes and a distinct aggregation phenomenon in these adhered platelets (Fig. 5B), indicating that the materials ACPs and ACPs-CS had no anti-platelet adhesion effect. Compared with the TPU blank control, platelet adhesion strongly decreased in TPU/ACPs-CS-Hep, TPU/ACPs-CS-PVS-Ag/ACPs-CS-Hep 1 wt%, TPU/ACPs-CS-PVS-Ag/ACPs-CS-Hep 3 wt% composite membranes (Fig. 5B). Furthermore, the platelet adhesion of TPU/ACPs-CS-PVS-Ag/ACPs-CS-Hep 3 wt% membrane was less than that of TPU/ACPs-CS-PVS-Ag/ACPs-CS-Hep 1 wt% membrane (Fig. 5B). These data confirm that the composite membranes with ACPs-CS-Hep have an excellent anti-platelet adhesion effect, which enhances with the increase of the content of ACPs-CS-Hep.

3.6 ACPs-CS-PVS-Ag and ACPs-CS-Hep had good blood compatibility and biological safety

The good biological safety and blood compatibility of ACPs-CS-PVS-Ag had been presented in our previous study.[10] Likewise, we conducted the hemolysis reaction and MTT assays to illustrate whether ACPs-CS-Hep could cause the erythrocyte fragmentation or cytotoxicity.

From Fig. 6A and B, the hemolytic reaction was simply notable in the deionized water group (the positive control), which was undetected in the normal saline group (the negative control). Besides, the hemolytic reaction remained unobserved for erythrocytes maintained in PBS (pH = 7.4) containing ACPs-CS-Hep of different concentrations for 3 h. These results indicated that ACPs-CS-Hep had good hemocompatibility. Moreover, the cytotoxicity of ACPs-CS-Hep to human normal heptical cell line (HL-7702) was investigated. As shown in Fig. 6C, little cytotoxicity appeared for the ACPs-CS-Hep concentration less than 1000 μg mL^{-1} when compared with the control group for the cell viability rate above 95%.

4. Discussion

ACPs are a kind of amphiphilic biomaterial obtained by yeast hydrolysis and have lots of functional groups, such as carboxyl groups on their surface, which make them disperse in different polar solutions by acting as a carrier. CS contains a large number of amino groups, and ACPs can combine CS to form ACPs-CS *via* amide reaction. The amino groups of the ACPs-CS combine Hep and PVS-Ag, respectively, to generate two functional CS bio-carbon materials ACPs-CS-Hep and ACPs-CS-PVS-Ag, which have antibacterial and anticoagulant properties, and are non-toxic to normal cells, as well as have good blood compatibility and biocompatibility. In this study, we combined different bio-carbon materials with TPU matrix to synthesize functional composite membranes. We show that the generated bio-carbon materials ACPs, ACPs-CS, ACPs-CS-PVS-Ag, ACPs-CS-Hep and ACPs-CS-PVS-Ag/ACPs-CS-Hep can be uniformly dispersed in the hydrophobic TPU matrix and can form uniform composite membranes with the TPU matrix. By detection of the hydrophilic and mechanical properties, we demonstrate that the TPU composite membranes containing ACPs content of less than 5 wt% show good hydrophilicity. The addition of ACPs of less than 5 wt% has no effect on the mechanical properties of the TPU composite membranes. Our data suggest that the TPU/ACPs-CS-PVS-Ag/ACPs-CS-Hep composite membrane has good mechanical properties and hydrophilicity.

Catheter-associated infections are common bacterial infections. Patients treated with medical catheters often suffer from microbial infection, manifested as fever and chills.[4,11,12] The main factors of the occurrence of catheter-related infections include microbial contamination of the catheter joint and surrounding skin and improper operation of pipe placement

personnel. The common pathogens of catheter-related infections include *S. aureus* and *C. albicans*.[12–14] Silver antibacterial agents are a type of inorganic antibacterial agents. Silver ions not only disrupt ion transport by destroying the plasma membrane potential on the surface of bacteria to affect ATP level but also affect the function of proteins by directly crossing the cell membrane, thereby inducing bacterial death.[15] Due to the strong bactericidal function of silver ions and their potential harm to the human body, silver nanoparticles and silver-carrying materials are used to exert the bactericidal effect at present.[16] Luo *et al.*[17] found that the hydroxyl region of cyclodextrin-based metal–organic framework can be used to reduce the silver ion precursor to nano silver and to deliver silver nanoparticles, which shows a good antibacterial effect. Chen *et al.*[18] reported that when silver nanoparticles are fixed in polymethyl methacrylate, the antibacterial activity of these silver nanoparticles on *E. coli* gradually enhances with the increase of nano silver content. When the content of nano silver was 3.0%, the antibacterial activity of the silver nanoparticles on *E. coli* is as high as 92%. Moreover, silver nanoparticles can significantly inhibit the formation of biofilm. By coating the surface of polyether ketone with different doses of silver nanoparticles *via* magnetron sputtering technology, Liu *et al.*[19] found that the roughness of the surface of the materials and the water contact angle increase with the augmentation of dose of silver nanoparticles, and these silver nanoparticles possess obvious antibacterial properties and no toxicity to cells. In this study, the generated TPU/ACPs-CS-PVS-Ag and TPU/ACPs-CS-PVS-Ag/ACPs-CS-Hep composite membranes have been demonstrated to have strong antibacterial and antiadhesion activities to (*S. aureus*, *E. coli*, *C. albicans* and MRSA bacteria). However, little antibacterial and antiadhesion effects were found in the TPU blank, TPU/ACPs, TPU/ACPs-CS and TPU/ACPs-CS-Hep composite membranes. These findings suggest that the TPU composite membranes carrying ACPs-CS-PVS-Ag has antibacterial activity. What's more, compared to AgNPs(2 wt%, 3 wt% or 5 wt% content of Ag-Nfbs respectively) reported in reported studies,[20,21] TPU/ACPs-CS-PVS-Ag/ACPs-CS-Hep 1 wt% exhibited superior antibacterial activity.

In clinical, when patients are treated with catheters, stimulation of catheters can induce intima damage of blood vessels and thus leads to thrombosis, thereby further causing catheter-associated thrombosis.[6,22,23] Hep is a common anticoagulant preparation in clinical, and heparinized biomaterials have a good application prospect in new medical materials.[24,25] There are two methods for material surface fixation of heparin, namely physical method and chemical grafting. The findings reported by Zhang *et al.*[26] documented that PVC materials deposited by heparin on the surface using the radio-frequency plasma technology can significantly prolong clotting time compared with uncoated controls. Additionally, single-walled carbon nanotubes grafted by heparin on their surface exhibit good anticoagulant activity.[27] Pan *et al.*[28] found that titanium materials fixed with PEG and Hep on the surface using a carbodiimide-based method for covalent coupling can significantly diminish the adsorption level of human plasma fibrinogen, inhibit platelet activation, prolong the activated partial thromboplastin time, and improve the blood compatibility of the material surface. TPU is a polymer material widely used in the field of medical devices such as catheter, which has good biocompatibility and mechanical properties. However, as a foreign material, TPU may still trigger the clotting process and cause thrombus.[29] A previous report showed that the TPU matrix grafted by heparin through covalent bonds can improve blood compatibility and delay blood coagulation.[30] Our results found that compared with the blank TPU, TPU/ACPs, and TPU/ACPs-CS membranes, the TPU composite membranes carrying ACPs-CS-Hep show distinct anticoagulant and anti-platelet adhesion effects. Moreover, the platelet adhesion of TPU/ACPs-CS-PVS-Ag/ACPs-CS-Hep 3 wt% membrane was less than that of TPU/ACPs-CS-PVS-Ag/ACPs-CS-Hep 1 wt% membrane, indicating that the anticoagulant activity enhances with the increase of the content of ACPs-CS-Hep. By combining the evaluation of hydrophilicity, mechanical properties, anticoagulant activity, and antibacterial function of the TPU/ACPs-CS-PVS-Ag/ACPs-CS-Hep membrane, we conclude that the optimal addition content of bio-carbon materials ACPs-CS-PVS-Ag and ACPs-CS-Hep is 1 wt%.

5. Conclusions

This study synthesizes ACPs derived TPU/ACPs-CS-PVS-Ag/ACPs-CS-Hep membrane *via* a simple preparation process. Our results indicated TPU/ACPs-CS-PVS-Ag/ACPs-CS-Hep possessed a good mechanical propertieswith strong anti-agglutinating and antibacterial effects, which may overcome the two major problems of thrombosis and bacterial infection of catheter. Collectively, our studies provides important research ideas for the development of antibacterial anticoagulant catheters.

Ethical statement

All experiments were performed in compliance with the regulations of ethical reviews of biomedical research involving human subjects. All human blood samples were obtained from Huaihe Hospital of Henan University and approved by the IRB of Huaihe Hospital of Henan University (Approval No.: 2024-03-028) and Biomedical Research Ethics Subcommittee of Henan University (Approval No.: HUSOM2025-574).

Author contributions

Zhang Wenxin and Geng Yanna designed the experiments. Wu Qiang supervised the project. Geng Yanna collected the human blood samples. Zhang Wenxin, Liu Shuai, Wang Xueping and Xu Xiaoke conducted the experiments. Zhang Wenxin, Geng Yanna, Wang Mengke and Wu Qiang analyzed the data. Zhang Wenxin, Geng Yanna and Wang Mengke prepared the manuscript. Wu Qiang, Zhang Wenxin, Geng Yanna and Wang Mengke revised the manuscript. All authors read the approved the final manuscript.

Conflicts of interest

There are no conflicts to declare.

Data availability

The data supporting this article have been included as the SI. See DOI: https://doi.org/10.1039/d5ra01833a.

Acknowledgements

This study was supported by the Henan Provincial Science and Technology Research Project (No. 242102230118).

Notes and references

1 B. Crooks, S. Harrison, G. Millward, K. Hall, M. Taylor, K. Farrer, A. Abraham, A. Teubner and S. Lal, *JPEN, J. Parenter. Enteral Nutr.*, 2022, **46**, 254–257.
2 C. Abbruzzese, A. Guzzardella, D. Consonni, G. Turconi, C. Bonetti, M. Brioni, M. Panigada and G. Grasselli, *Ann. Intensive Care*, 2023, **13**, 106.
3 H. M. Li, L. L. Wan, C. X. Jin, G. Y. Zhang, H. Yang and X. Y. Zhang, *BMC Infect. Dis.*, 2023, **23**, 603.
4 K. Moriyama, T. Ando, M. Kotani, J. Tokumine, H. Nakazawa, A. Motoyasu and T. Yorozu, *Medicine*, 2022, **101**, e31160.
5 X. Liu, H. Ye, X. Zheng, Z. Zheng, W. Chen and X. Yu, *Hemodial. Int.*, 2022, **26**, 13–22.
6 J. C. Laguna, T. Cooksley, S. Ahn, N. Tsoukalas, T. H. Oo, N. Brito-Dellan, F. Esposito, C. Escalante and C. Font, *Support. Care Cancer*, 2022, **30**, 8577–8588.
7 D. W. Gould, J. Doidge, M. Z. Sadique, M. Borthwick, R. Hatch, F. J. Caskey, L. Forni, R. F. Lawrence, C. MacEwen, M. Ostermann, P. R. Mouncey, D. A. Harrison, K. M. Rowan, J. D. Young and P. J. Watkinson, *Health Technol. Assess.*, 2022, **26**, 1–58.
8 H. Shao, T. Zhang, Y. Gong and Y. He, *Adv. Healthcare Mater.*, 2023, **12**, e2300932.
9 M. Nituica, O. Oprea, M. D. Stelescu, M. Sonmez, M. Georgescu, L. Alexandrescu and L. Motelica, *Materials*, 2023, **16**(15), 5279.
10 Y. Geng, S. Liu, M. Wang, X. Wang and Q. Wu, *J. Exp. Nanosci.*, 2024, **19**(1), 2336242.
11 G. Louis, T. Belveyre, A. Jacquot, H. Hochard, N. Aissa, A. Kimmoun, C. Goetz, B. Levy and E. Novy, *BMC Infect. Dis.*, 2021, **21**, 534.
12 J. Phillips, D. T. Chan, A. Chakera, R. Swaminathan, K. Patankar, N. Boudville and W. H. Lim, *Nephrology*, 2023, **28**, 249–253.
13 K. M. Chow, P. K. Li, Y. Cho, A. Abu-Alfa, S. Bavanandan, E. A. Brown, B. Cullis, D. Edwards, I. Ethier, H. Hurst, Y. Ito, T. P. de Moraes, J. Morelle, N. Runnegar, A. Saxena, S. W. So, N. Tian and D. W. Johnson, *Peritoneal Dial. Int.*, 2023, **43**, 201–219.
14 B. S. Rabelo, K. A. F. de Alvarenga, J. Miranda, T. P. Fagundes, C. S. P. Cancela, R. M. de Castro Romanelli and K. E. de Sá Rodrigues, *Am. J. Infect. Control*, 2023, **51**, 99–106.
15 R. Sharma and N. Srivastava, *Anti-Cancer Agents Med. Chem.*, 2021, **21**, 1793–1801.
16 R. A. Dorgham, M. N. Abd Al Moaty, K. P. Chong and B. H. Elwakil, *Int. J. Mol. Sci.*, 2022, **23**(18), 10243.
17 T. Luo, S. Shakya, P. Mittal, X. Ren, T. Guo, M. G. Bello, L. Wu, H. Li, W. Zhu, B. Regmi and J. Zhang, *Int. J. Pharm.*, 2020, **584**, 119407.
18 X. Chen, T. Yan, S. Sun, A. Li and X. Wang, *Front. Cell. Infect. Microbiol.*, 2023, **13**, 1325103.
19 X. Liu, K. Gan, H. Liu, X. Song, T. Chen and C. Liu, *Dent. Mater.*, 2017, **33**, e348–e360.
20 A. Gudimalla, J. Jose, R. J. Varghese and S. Thomas, *J. Polym. Environ.*, 2021, **29**, 1412–1423.
21 P. A. Zapata, M. Larrea, L. Tamayo, F. M. Rabagliati, M. I. Azócar and M. Páez, *Mater. Sci. Eng., C*, 2016, **69**, 1282–1289.
22 F. Pinelli and P. Balsorano, *J. Vasc. Access*, 2020, **21**, 405–407.
23 J. Szymańska, K. Kakareko, A. Rydzewska-Rosołowska, I. Głowińska and T. Hryszko, *J. Clin. Med.*, 2021, **10**(11), 2230.
24 A. Lawanprasert, S. Pimcharoen, S. E. Sumner, C. T. Watson, K. B. Manning, G. S. Kirimanjeswara and S. H. Medina, *Small*, 2022, **18**, e2203751.
25 E. Pilia, A. Belletti, S. Fresilli, T. C. Lee, A. Zangrillo, G. Finco and G. Landoni, *Lung*, 2023, **201**, 135–147.
26 Y. Zhang, J. Man, J. Wang, J. Liu, X. Song, X. Yu, J. Li, R. Li, Y. Qiu, J. Li and Y. Chen, *Int. J. Biol. Macromol.*, 2024, **254**, 127653.
27 L. Y. Yan, W. Li, X. F. Fan, L. Wei, Y. Chen, J. L. Kuo, L. J. Li, S. K. Kwak, Y. Mu and M. B. Chan-Park, *Small*, 2010, **6**, 110–118.
28 C. J. Pan, Y. H. Hou, B. B. Zhang, Y. X. Dong and H. Y. Ding, *J. Mater. Chem. B*, 2014, **2**, 892–902.
29 J. Oh, Y. K. Kim, S. H. Hwang, H. C. Kim, J. H. Jung, C. H. Jeon, J. Kim and S. K. Lim, *Polymers*, 2022, **14**(10), 2033.
30 K. D. Park, T. Okano, C. Nojiri and S. W. Kim, *J. Biomed. Mater. Res.*, 1988, **22**, 977–992.